exposed HeLa cells in vitro (*2*). Our Reflectoscope results, however, are inconsistent with those reported for similarly treated human lymphocytes in vitro (*1*). We have no explanation for the discrepancy. In both cases, however, the positive control (mitomycin C) yielded significantly more SCE's.

In an initial attempt to verify the positive results of Liebeskind *et al.* (*1*), in vitro whole blood was exposed to ultrasound under conditions similar to theirs, but our results were negative (*7*). To better approximate their exposure conditions, lymphocytes obtained by gravity sedimentation were exposed to intensities of ultrasound that spanned those used by Liebeskind *et al.* (*1*). The results were again negative (*5*). Experiments were then conducted with continuous-wave ultrasound from an experimental unit under conditions that induced a small but significant amount of cell destruction: among the surviving cells there was no increase in the frequency of SCE's.

In experiment 1, the same ultrasound devices and cell culture facilities as used earlier (*1, 2*) were used, as were the same general procedures (for example, Parafilm cover, blood composition, one common donor, exposure intensities), yet the results were negative. Experiment 2 included the same culture medium (McCoy's 5A) used by Liebeskind *et al.* (*1*), as well as the same time of BrdU addition, and the results were also negative.

The positive results of Liebeskind *et al.* (*1*) have not been verified. We conclude that the reasons for their obtaining such results may be coincident with some subtle yet unidentified procedural factor.

V. CIARAVINO
*Department of Radiation Biology and Biophysics, School of Medicine and Dentistry, University of Rochester, Rochester, New York 14642*
A. BRULFERT
*Laboratoire de Biologie Cellulaire, Faculté de Sciences Pharmaceutiques et Biologiques, University René Descartes, 75270 Paris Cedex 06 France*
M. W. MILLER
*Department of Radiation Biology and Biophysics, School of Medicine and Dentistry, University of Rochester*
D. JACOBSON-KRAM
*Department of Radiology, George Washington University School of Medicine, Washington, D.C. 20037*
W. F. MORGAN
*Laboratory of Radiobiology and Environmental Health, University of California, San Francisco 94143*

**References and Notes**

1. D. Liebeskind *et al.*, *Science* **205**, 1273 (1979).
2. D. Liebeskind *et al.*, *Radiology* **131**, 177 (1979).
3. S. B. Barnett, R. S. V. Baker, S. Barnstable, paper presented at the Third World Federation of Ultrasound in Medicine and Biology Congress, Brighton, England, July 1982.
4. C. A. Ehlinger, P. Katayama, M. R. Roesler, R. F. Mattingly, *Wis. Med. J.* **81**, 21 (1981); M. Haupt *et al.*, *Hum. Genet.* **39**, 221 (1981).
5. A. Brulfert, V. Ciaravino, M. W. Miller, E. L. Carstensen, *Ultrasound Med. Biol.* **10**, 309 (1984).
6. M. Lundberg *et al.*, *Am. J. Med. Genet.* **11**, 31 (1982).
7. M. W. Miller *et al.*, *Mutat. Res.* **120**, 261 (1983).
8. S. M. Morris, C. G. Palmer, F. J. Fry, L. K. Johnson, *Ultrasound Med. Biol.* **4**, 253 (1978); H. Z. Zheng, N. S. Mitter, A. E. Chudley, *ICRS J. Med. Sci.* **9**, 941 (1981).
9. P. Perry and S. Wolff, *Nature (London)* **251**, 156 (1974).
10. K. Morimoto and S. Wolff, *ibid.* **288**, 604 (1982); R. Tice, E. L. Schneider, J. M. Rary, *Exp. Cell. Res.* **102**, 232 (1976).
11. We thank R. Bases for the cooperation and hospitality offered to V.C. and A.B. during their stay at the Albert Einstein College of Medicine. We also thank P. N. Goodwin for his ultrasound dosimetry determinations. Supported by PHS grants GM22680, ES03238, and ES03000. This report is based on work performed partially under contract DE-AC02-76EV03490 with the U.S. Department of Energy and has been assigned report number DOE/EV/03490/2358.

8 November 1984; accepted 4 December 1984

# A Renal Countercurrent System in Marine Elasmobranch Fish: A Computer-Assisted Reconstruction

Abstract. *Computer-aided techniques were used to reconstruct the complex renal tubular system in the dorsal kidney region of a marine elasmobranch fish, the little skate (*Raja erinacea*), from a series of light micrographs of serial sections. It was established that five individual segments of one nephron, consisting of two loops and a distal tubule, are arranged in parallel within an elongated closed tissue sac. Capillaries, which form a network around these nephron segments, enter and exit this sac at the same end. This anatomical arrangement suggests that a complex renal countercurrent multiplier system may be important in fluid regulation in these fish.*

Typically, marine fish are faced with the problem of dehydration due to the high osmolality of the surrounding seawater (*1*). Marine elasmobranch fish appear to resolve the problem by maintaining high urea concentrations in plasma and tissue, thereby elevating the osmolality of their internal milieu to nearly that of the surrounding seawater (*2*). An extremely small fraction of urea is excreted (*3*), and studies of the kidney have been done to determine how this urea conservation is achieved (*1–5*). However, the extremely complex configuration of the elasmobranch nephron has impeded physiological studies of the anatomical site of urea reabsorption and of some of the cellular mechanisms that are involved (*6*). This nephron complexity is evidenced by the fact that elasmobranchs are members of the only vertebrate class (Chondrichthyes) in which the nephron configuration and epithelial sequence along its length to the collecting duct are not known (*6, 7*).

We used computer graphics to study nephron configuration. A three-dimensional reconstruction of the tubule in the complex dorsal region of a marine elasmobranch kidney shows that parallel tubular segments from a single nephron are tightly wrapped in a cellular sheath that also encloses a capillary network around the tubules. This anatomical arrangement presumably has the potential of facilitating a physiological countercurrent system.

The kidneys of little skates (*Raja erinacea*) and spiny dogfish (*Squalus acanthias*) were fixed with buffered glutaraldehyde by vascular perfusion (*8*). We used 118 light micrographs of serial sections from the skate to outline and sequence 2945 tubule contours (outer circumference of tubules) of the sectioned nephron as it completed its course within the dorsal region of the kidney. The same photographs were used to outline the cellular peritubular sheath that surrounds bundles of these tubule segments (*9*). Because a complex computer-generated image was expected, the profiles of the blood vessels accompanying the tubules were not entered into the computer. The course of these vessels was simpler than that of the adjacent tubules and it was traced in the same serial sections by light microscopy.

The architectural complexity of nephrons in the dorsal region was greater than what could be reconstructed by techniques such as wax modeling. For the computer-assisted reconstruction, we used a hierarchical data-base design that accommodates the complex branching nature of biological structures and performs coordinate transformations necessary to convert serially sectioned biological materials into three-dimensional display coordinates. Solid modeling algorithms were used to generate the video images (*10, 11*).

Beginning with the urinary pole of the renal corpuscle, we traced the course of the nephron as it first entered the bundle zone in the dorsal region of the kidney

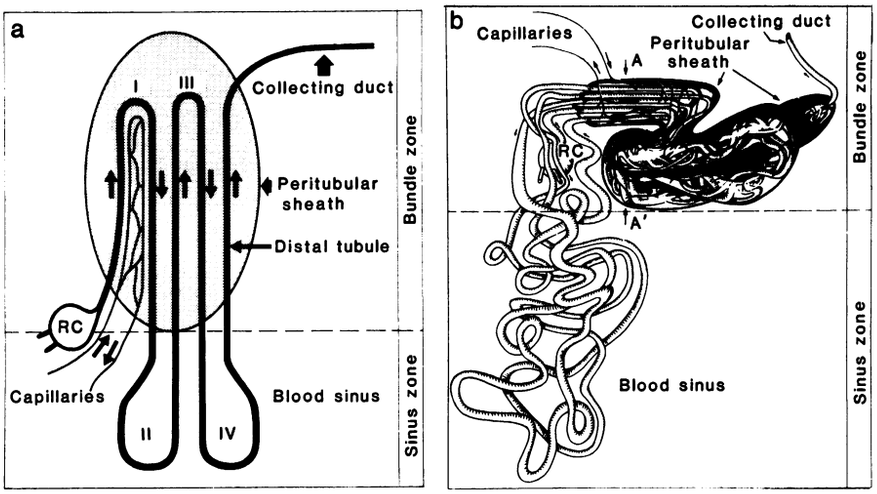


Fig. 1. Diagrams of elasmobranch nephron in the bundle zone (dorsal) and sinus zone (ventral). The dorsal kidney surface is parallel to the top of the page. (a) Simplified diagram showing renal corpuscle (RC) and four highly stylized nephron loops (I to IV). A peritubular sheath surrounds the countercurrent system of nephron segments (loops I, III, and the distal tubule) and anastomosing capillary loops in the bundle zone. Small arrows indicate the direction of tubular fluid and blood flow. (b) Schematic drawing of the pathway of the skate nephron in the bundle zone (dorsal) and in the sinus zone (ventral) showing some of the nephron complexity. The entering limbs of nephron loops I and III and the distal tubule (a) pierce the peritubular sheath near the renal corpuscle and extend to the opposite end of the sheath. Close to the renal corpuscle, the five tubular segments (loops I, III, and the distal tubule) located in the bundle zone are covered by the peritubular sheath and run parallel to each other. To emphasize this distinctive course, they have been drawn side by side in one plane and not assembled into a bundle, as they actually are (Figs. 2 and 3). The tubular bundle and surrounding peritubular sheath then become convoluted. The parallel course of the tubules is lost since the loops wrap around each other. For simplicity, the opposite end of the peritubular sheath, where the distal tubule emerges, has been drawn away from the renal corpuscle on the far right side of the diagram. The distal tubule pierces the sheath at this point to join a collecting duct, whereas the two other nephron segments loop back and retrace their path, finally exiting the sheath where they entered it. Capillaries also enter and exit the peritubular sheath at its renal corpuscle terminus and form an anastomotic network around and within the tubular bundle. A histological section perpendicular to the plane of the drawing and along the line A–A′ is shown in Fig. 2. In the sinus zone, loops II and IV meander in large blood sinuses.

and made the first of four large loops (Fig. 1). After forming a first dorsal loop, the tubule turned and exited the bundle zone to reach the sinus zone in the ventral part of the kidney. There the nephron formed a second loop (loop II in Fig. 1), returned to the bundle zone, and with a third loop (loop III in Fig. 1) returned to the sinus zone. Finally, after a fourth loop (loop IV in Fig. 1), the nephron reentered the bundle zone and, as the distal tubule, it joined a collecting duct in the subcapsular region. In the bundle zone, both loops I and III (each composed of two limbs, one ascending and one descending) and the early distal tubule are close together (Fig. 1a). This bundle of five tubular segments, all from the same nephron, was wrapped by a cellular peritubular sheath separating them from other peritubular sheaths (each containing two nephron loops and an early distal tubule) derived from other nephrons (Figs. 1 and 2). The peritubular sheath (Figs. 1 and 2) was observed to be an elongated closed sac formed by sever-

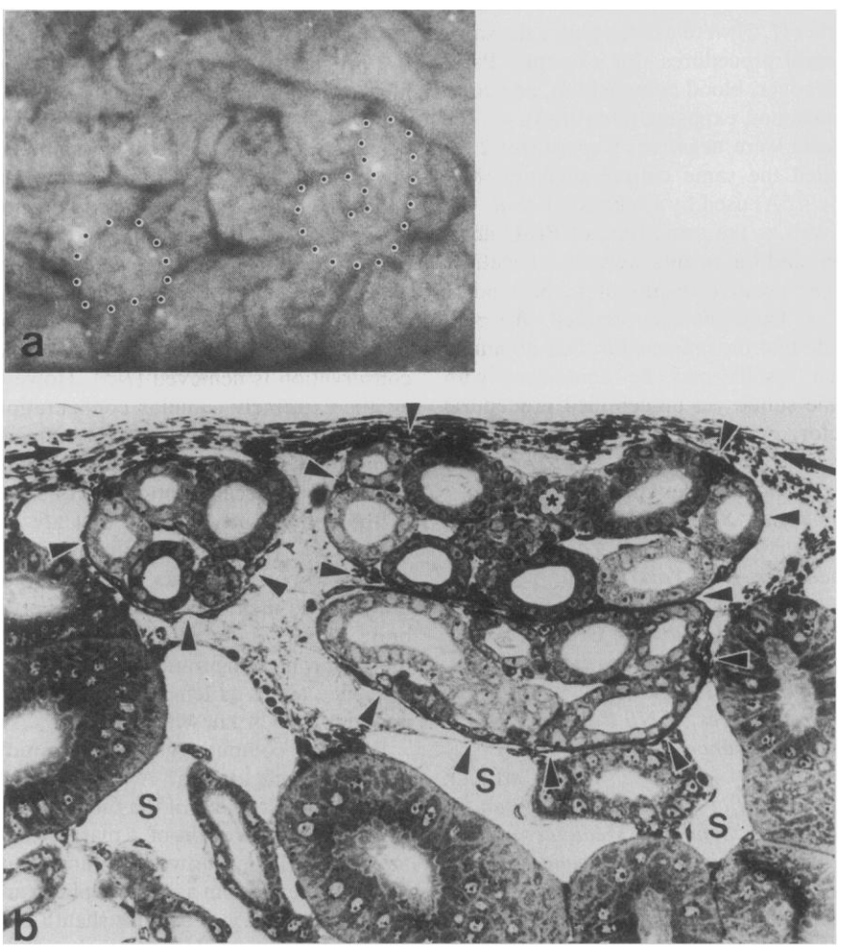


Fig. 2. (a) Photomicrograph of dorsal skate kidney surface showing a field of numerous tightly intertwined nephron segments. Two discrete tubular bundles are outlined, with nephrons visible through the peritubular sheath. The tubular bundle here corresponds to the reconstructed tubular bundle shown in Fig. 3d. (b) Photomicrograph of epoxy resin section cut through the dorsal region of skate kidney in a plane similar to that along A–A′ in Fig. 1b. Three regions of the same tubular bundle and surrounding peritubular sheath (arrowheads) in the bundle zone are shown. On the upper left are five cross-sectional nephron segments and capillaries (small white areas between tubules) of the straight part of the countercurrent system. On the upper right, the tubules in the peritubular sheath are looping back so that those on the right are continuous with those on the left (star). Just below this, on the right, the sheath (arrowheads) encloses capillaries and the five tubules cut in a convoluted part of the tubule bundle. S, individual tubules in the sinus zone. Arrows indicate the dorsal kidney capsule. Magnification, ×200.

al investing layers of squamous cells that surround the tubules. Freeze-fracture and thin sections have shown tight junctions between adjacent squamous cells of the peritubular sheath. This peritubular sheath was penetrated on one end, near the renal corpuscle, by entering and exiting tubule segments of the two nephron loops and distal tubule and by capillaries that formed an anastomosing network around these five tubule segments (Fig. 1). At the opposite end, the peritubular sheath was pierced only by the exiting distal tubule. In contrast, the segments of the nephron in the sinus zone of the kidney were less organized and were not surrounded by a peritubular sheath but instead intermingled randomly with other nephron segments in large blood sinuses (Figs. 1 and 2).

In our reconstructed images of the skate nephron (Fig. 3), this bundle of five tubules (ascending and descending limbs of nephron loops I, III, and the early distal tubule as diagrammed in Fig. 1a) and the surrounding peritubular sheath (Fig. 3) continued in a straight course from near the renal corpuscle just under the skate kidney surface for approximately 0.25 mm (285 μm). The tubules within the straight part of the peritubular sheath were arranged in a parallel fashion. The peritubular sheath then became convoluted, twisting back under the straight portion of the sheath and making several additional turns. The convoluted part of the peritubular sheath was slightly more than 3 mm long (3163 μm) in the skate, as determined from the reconstructed path length. The nephron segments within the convoluted part of the sheath also became somewhat convoluted as they wound around each other, and the strict parallelism observed in the straight part of the sheath was not maintained (Fig. 3). The total path length of nephron loops I, III, and the early distal tubule were 4902, 8247, and 3636 μm, respectively (*12*). Capillaries observed in the histological sections entered and exited the end of the peritubular sheath along with the tubules, as shown in Fig. 1b. The capillaries formed an anastomotic network around and within the tubular

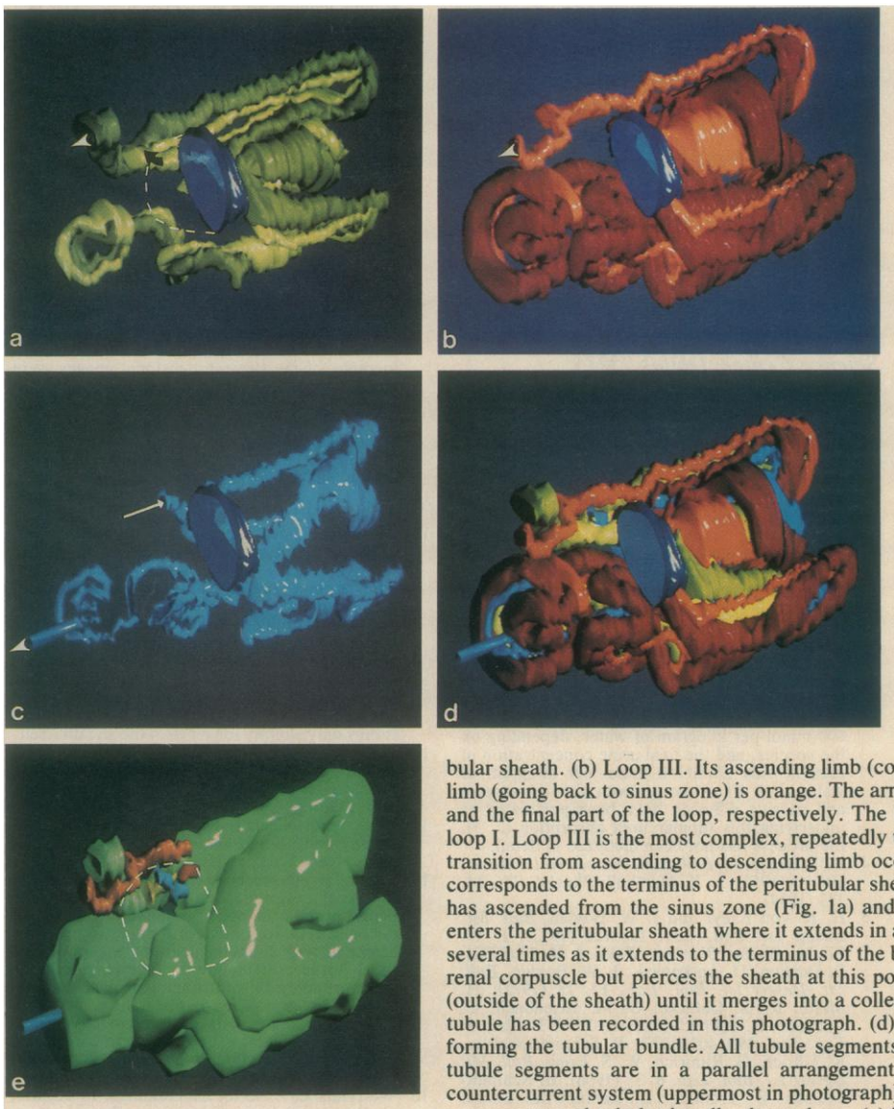


Fig. 3. Computer reconstruction of skate tubular bundle in the bundle zone (dorsal region) and its peritubular sheath. All segments shown are part of the same nephron. The dark blue calotte-shaped structure is part of the renal corpuscle close to the urinary pole. For better visualization of the tubules, the remainder of the renal corpuscle [dashed line in (a)] has not been reconstructed here. The straight part of the countercurrent system is uppermost in each photograph, as is the dorsal kidney surface. In these reconstructions the terminus of the peritubular sheath is in the lower left corner of each photograph. (a) Loop I (see Fig. 1a). The ascending (entering) limb is light green and the descending (exiting) limb is dark green. The arrow is in the ascending limb, close to its starting point from the urinary pole of the renal corpuscle, which is hidden in this perspective. After emerging from the renal corpuscle, the tubule goes left and then turns sharply right and runs along the straight part of the countercurrent system. At the upper right, the ascending limb bends back and after numerous convolutions turns to become the descending limb. The transition from ascending to descending limb occurs at the lower left of photograph. The limbs are tightly wrapped around each other as the descending limb retraces the path of the ascending limb. The arrowhead is in the final part of the loop after it has exited the peritubular sheath. (b) Loop III. Its ascending limb (coming from sinus zone) is red and its descending limb (going back to sinus zone) is orange. The arrow and arrowhead are in the beginning segment and the final part of the loop, respectively. The basic pattern of this loop is the same as that of loop I. Loop III is the most complex, repeatedly turning and wrapping itself tightly together. The transition from ascending to descending limb occurs at the lower left of the photograph, which corresponds to the terminus of the peritubular sheath (d). (c) Distal tubule. This nephron segment has ascended from the sinus zone (Fig. 1a) and starts close to the renal corpuscle (arrow). It enters the peritubular sheath where it extends in a straight path as the early distal tubule. It turns several times as it extends to the terminus of the bundle (arrowhead). It does not loop back to the renal corpuscle but pierces the sheath at this point, where it continues as the late distal tubule (outside of the sheath) until it merges into a collecting duct. Only the initial part of the late distal tubule has been recorded in this photograph. (d) Composite of loops I, II, and the distal tubule forming the tubular bundle. All tubule segments have the same positions as in (a) to (c). The tubule segments are in a parallel arrangement along the length of the straight part of the countercurrent system (uppermost in photograph). Each outlined bundle of Fig 2a corresponds to a reconstructed tubular bundle shown here. (e) The peritubular sheath surrounding the tubular bundle. The renal corpuscle has been removed and is outlined by dashes. The perspective is the same as in (a) to (d). The closed end of the sheath near the renal corpuscle is pierced by the five tubular segments: entering and exiting limbs of loops I (light green and dark green) and III (red and orange) and the entering distal tubule (blue), where the straight part of the countercurrent system begins. The early distal tubule (inside the sheath) exits the sheath at its terminus in the lower left corner of the photograph, where it becomes the late distal tubule. After the straight part of the countercurrent system (upper right) the numerous turns of the tubular bundle are more easily visualized by the large sweeping turns of the peritubular sheath. Capillaries are not reconstructed here but would enter and exit the peritubular sheath near the renal corpuscle as shown in Fig. 1b.

bundle as they extended to the end of the sheath. Serial sections of the shark kidney, although not used for computer graphics, showed tubule bundles (each wrapped by a peritubular sheath) composed of linearly arranged nephron segments and capillaries like those in the skate.

This parallel arrangement of tubules and capillaries has the potential to operate as a countercurrent multiplier system. The complete countercurrent flow system consists of a straight bundle of five tightly packed tubules from a single nephron, three of which pass in one direction and two of which travel counter to that direction. Among the tubules there is a system of anastomosing capillaries that also run the length of the tubular bundle. Both tubules and capillaries are encased by the peritubular sheath.

Tubular fluid from the glomerular ultrafiltrate travels in the same direction in the ascending limb of the first loop (I) as tubular fluid in the ascending limb of the third loop (III) and the tubular fluid in the distal tubule (Fig. 1). Countercurrent flow occurs in the descending limbs of both dorsal loops (I and III). The dual character of the system, in which the two countercurrent flows are parallel to one another, is unusual. Presumably fluid within the space contained by the peritubular sheath is shared by the exterior of the five enclosed tubules and capillaries.

Similarities to mammalian kidney structure suggest that marine elasmobranch fish may employ renal countercurrent mechanisms to achieve osmotic balance. The mammalian kidney is arranged so that descending and ascending loops of Henle and collecting ducts share extracellular fluid in the renal medulla, which contains a network of descending and ascending capillaries. In these fish, the peritubular sheath probably seals each bundle of five tubules and associated capillaries from the rest of the organ, thus forming a discrete anatomical unit. This may create some functional similarities to the conditions within the mammalian renal medulla, in which there is a net reabsorption and subsequent recycling of urea (*13*). However, the renal countercurrent multiplier system in mammals, which has the capacity to produce a hypertonic urine as well as to reabsorb most urea, must be significantly different from that of the elasmobranch kidney, which conserves urea but does not produce an osmotically concentrated urine (*1, 2*). Furthermore, finding the anatomical requisites for a renal countercurrent multiplier system in elasmobranch fish is surprising in that the presence of such a system in both birds and mammals mainly facilitates the ability to form an osmotically concentrated urine (*14*). The precise fluid and solute transfers that occur at each segment in the elasmobranch renal tubular system have not yet been established, and we cannot specify, on the basis of anatomical reconstruction alone, how a countercurrent mechanism would work, Ultrastructural studies indicate, however, that the tubular epithelial cells are diverse within the various segments of the tubules (*15*) and have the potential for active transport of solutes. Integration of such information into a realistic model for fluid and solute transfers is an objective for future studies.

ERIC R. LACY
*Department of Anatomy, Harvard Medical School, Boston, Massachusetts 02115,* and *Laboratory of Electronmicroscopy, Hannover Medical School, 3000 Hannover, Federal Republic of Germany*
ENRICO REALE
*Laboratory of Electronmicroscopy, Hannover Medical School*
DANIEL S. SCHLUSSELBERG
WADE K. SMITH
DONALD J. WOODWARD
*Department of Cell Biology and Physiology, University of Texas Health Science Center, Dallas 75235*

### References and Notes

1. H. W. Smith, *Am. J. Physiol.* **98**, 296 (1931).
2. _____, *Biol. Rev. Cambridge Phil. Soc.* **11**, 49 (1936).
3. Marine elasmobranchs have mechanisms that allow their body fluids to be nearly isosmotic with seawater, thus preventing major fluxes of water into or out of their tissues. Although both sodium and chloride ions are abundant in the plasma, they are excreted in equally high concentrations (*1*). Urea and, to a lesser extent, trimethylamine oxide account for most of the elevated osmolality of the internal milieu of these fish (*2*). Urea is conserved since about 90 percent of that filtered through the glomerulus is reabsorbed within the nephron (*2, 4*). Plasma concentrations of urea range between 300 and 600 mmol per kilogram of water, depending on the species, and the final urine concentration of urea is only about 50 mmol per kilogram of water (*1, 2, 4*). Although both active transport and passive diffusion have been postulated as underlying this tubular urea absorption (*2, 5*), the process has not been analyzed in detail.
4. R. T. Kempton, *Biol. Bull. (Woods Hole, Mass.)* **104**, 45 (1953); E. K. Marshall, *Physiol. Rev.* **14**, 133 (1934).
5. H. R. von Baeyr and J. W. Boylan, *Bull. Mt. Desert Isl. Biol. Lab.* **13**, 121 (1973); J. W. Boylan, *Comp. Biochem. Physiol.* **42**, 27 (1972); P. Deetjen, D. Antkowiak, J. W. Boylan, *Bull. Mt. Desert Isl. Biol. Lab.* **12**, 28 (1972); H. Stolte, R. G. Galaske, G. M. Eisenbach, C. Lechene, B. Schmidt-Nielsen, J. W. Boylan, *J. Exp. Zool.* **199**, 403 (1977); B. Schmidt-Nielsen, K. Ullrich, G. Rumrich, W. S. Long, *Bull. Mt. Desert Isl. Biol. Lab.* **6**, 35 (1966); B. Schmidt-Nielsen, B. Truniger, L. Rabinowitz, *Comp. Biochem. Physiol. A* **42**, 13 (1972).
6. The elasmobranch nephron is one of the most complex among vertebrates (*4, 5*). Tissue maceration and tubular lumen dye injection studies have provided some details of nephron configuration, but the highly tortuous path of the tubule has made a complete description of the nephron difficult. This in turn has prevented accurate tubular fluid sampling by micropuncture since the puncture site cannot be conclusively identified. Although a peculiar parallel arrangement of some nephron segments was reported in earlier studies (*5, 7*), each proposed model of this part of the elasmobranch nephron has been inferred either from partial injection of nephrons or from time-lapse cinematography, which does not allow determination of the exact location of tubules that may appear to be adjacent at the low magnifications used. All of the models have therefore been significantly different (*2, 5, 7*). Thus, the tubular site for this urea conservation has awaited more detailed morphological analysis.
7. E. Borghese, *Z. Zellforsch. Mikrosk. Anat.* **72**, 88 (1966); P. Deetjen and D. Antkowiak, *Bull. Mt. Desert Isl. Biol. Lab.* **10**, 5 (1970); P. Deetjen and J. Boylan, *ibid.* **8**, 16 (1968); R. T. Kempton, *J. Morphol.* **73**, 147 (1943); *ibid.* **111**, 217 (1953); E. R. Lacy, B. Schmidt-Nielsen, R. G. Galaske, H. Stolte, *Bull Mt. Desert Isl. Biol. Lab.* **5**, 54 (1975); K. Thurau and P. Acquisto, *ibid.* **9**, 60 (1969).
8. Fixed renal tissue was embedded in epoxy resin, and 1-μm-thick sections were stained with toluidine blue and photographed with the light microscope.
9. There was an average of 5.7 μm of tissue between successive photographs, which were enlarged approximately 250 diameters.
10. The outer contour of each tubule profile in each photograph and of the peritubular tissue sheath in every fifth photograph was traced on a digital graphic tablet with a hand-held stylus. The tablet drove a user-defined cursor for digitized images which were stored in a 16-bit minicomputer (Data General Eclipse S/130); this was interfaced to a microprogrammable graphics processor (Adage 3000) for rapid image construction and analysis. Microcoded programs were used for rapid vector generation and smooth-shaped polygon filling of high-resolution images (1000 by 1000 pixels). Video graphics images were used to align contours from serial sections. The graphic data base was used to reconstruct long tubes from individual contours. A set of contours was then subjected to a surfacing routine, which generated triangles between the contours (*11*). By combining output of a lighting algorithm with perspective calculations, polygon fill, and Z-buffer hidden-surface techniques, we constructed a view of the three-dimensional surface of the skate nephron. Photographs of the three-dimensional images were made directly from the video screen. See *Computer Graphics World* (Pennwell, Tulsa, Okla., May 1983) and *Electronics Imaging* (Morgan-Grampion, Boston, 1983), pp. 26–32, for color illustrations of a range of familiar biological objects imaged by these methods.
11. H. Fuchs, Z. M. Kedem, S. Uselton, *Commun. ACM* **20**, 693 (1977).
12. All segments of the nephron in the straight part of the peritubular sheath were 285 μm long since the five tubules were in strictly parallel alignment. Loop I did not extend to the terminus of the peritubular sheath, whereas loop III (Fig. 1a) not only extended to the terminus of the peritubular sheath but was continuously wrapped around loop I and the early distal tubule; this accounts for its length of more than 8 mm. The early distal tubule took a virtually straight course in the convoluted part of the sheath and is thus only slightly longer than the sheath itself.
13. J. R. Clapp, *Am. J. Physiol.* **210**, 1304 (1966); W. E. Lassiter, M. Mylle, C. W. Gottschalk, *ibid.*, p. 965; F. Roch-Ramel, F. Chomety, G. Peters, *ibid.* **215**, 429 (1970).
14. K. Schmidt-Nielsen, *Animal Physiology: Adaptation and Environment* (Cambridge Univ. Press, New York, 1975).
15. The following successive segments beginning at the renal corpuscle can be observed in each nephron: (i) the neck segment consisting of cuboidal cells with numerous cilia; (ii) proximal segments with epithelial cells characterized by a brush border; (iii) an intermediate segment, with six morphologically distinct portions; and (iv) the distal segments (early distal in the peritubular sheath and late distal in the connective tissue outside the sheath). The distal segment merges into the collecting duct, which extends to larger collecting tubules.
16. We thank C. Colette, L. Trakimas, F. Köhler, G. Pugh, and B. McOwen for technical assistance. Supported by the Alexander von Humboldt Foundation and the National Institutes of Health (grant AM-06345) (E.R.L.), Deutsche Forschungsgemeinschaft (Sonderforschungsbereich 146) (E.R.), the Biological Humanics Foundation (D.J.W.), and by the National Institute of Alcohol Abuse and Alcoholism (D.S.S.).

7 September 1984; accepted 1 November 1984